CrystEngComm

Accepted Manuscript

ROYAL SOCIETY OF CHEMISTRY

www.rsc.org/crystengcomm

Cite this: DOI: 10.1039/c0xx00000x

www.rsc.org/xxxxxx

ARTICLE TYPE

Synthesis of Metal-Organic Framework Particles and Thin Films *via* Nanoscopic Metal Oxide Precursors

Yanfeng Yue,[*a] Nada Mehio,[b] Andrew J. Binder,[b] and Sheng Dai[*ab]

Received (in XXX, XXX) Xth XXXXXXXXX 20XX, Accepted Xth XXXXXXXXX 20XX

DOI: 10.1039/b000000x

Metal-organic frameworks (MOFs) are a diverse family of hybrid inorganic–organic crystalline solids synthesized by assembling secondary building units (SBUs) and organic ligands into a periodic and porous framework. Microporous MOF materials, due to their high permeability and size selectivity, have attracted tremendous interest in gas storage and separation, large molecule adsorption, catalysis, and sensing. Despite the significant fabrication challenges, nanosized MOF particles can be fabricated to display enhanced gas storage and separation abilities in comparison to the parent MOF bulk counterparts under special synthesis conditions. So far, the majority of MOF nanocrystals have been derived from the controlled nucleation and growth of molecular precursors in homogeneous solutions. However, synthesis protocols based on nucleation and growth from dilute solution precursors are difficult to adapt to the synthesis of other nanoscopic materials, such as thin film and mixed-matrix membranes, which limits the practical applications of MOFs. This article discusses the current status of synthetic methods that have been utilized to fabricate MOF-based nanoscopic materials and ultrathin membranes from nanoscopic metal oxide precursors.

1. Introduction

Metal-organic frameworks (MOFs) are a diverse family of hybrid inorganic–organic crystalline solids in which secondary building units (SBUs) are assembled to form a periodic and porous framework. A SBU assembly affords exquisite control over pore shape and connectivity.[1,2] This is due to the fact that the SBU assembly is strongly dependent on the coordination preference of the metal ion and the length and rigidity of the oligotopic organic linkers. Compared to the bulk MOF materials, nanometer-sized MOFs (nanoMOFs) have attracted considerable attention because of their potential applications in drug delivery, catalysis, and separation.[3–4] In particular, highly porous MOF materials have been used as chemical sensors for the detection of gas and vapor phase analytes.[5] So far, a significant number of research studies have been devoted to the preparation of nanoMOF materials; however, the majority of those studies derive MOF nanocrystals from the controlled nucleation and growth of molecular precursors in a homogeneous solution.[6] Although synthesizing MOF nanocrystals from soluble metal salt precursors appear to be simple, the reaction conditions must be tightly controlled. Moreover, synthesis protocols based on nucleation and growth from dissoluble metal salt precursors are difficult to adapt to the synthesis of MOF thin films, which limits the practical applications of MOFs. Specifically, it limits the utility of MOFs to a number of areas of research in which MOFs are promising candidates, such as continuous membrane based separations, membrane reactors, and a wide variety of optical, electronic, catalytic, and magnetic nanodevices.

Since MOF materials exhibit oriented and well-defined structures, they are amenable to being processed as thin films. Until recently, two basic synthetic schemes have been applied to MOF membrane fabrication: an *in situ* synthetic approach and a secondary-growth method.[7,8] The *in situ* approach is essential to promoting the growth of crystalline materials on bare or chemically modified supports via a one-step, one-pot solvothermal method. On the other hand, the secondary-growth method is designed to fix small nanosized MOF seeds to a support surface in the first step and subsequently, grow a continuous polycrystalline layer under solvothermal conditions in the second step. However, in recent years, an alternative synthetic scheme based on the nanoscale-facilitated transformation of nanosized metal oxide precursors has been reported in the literature.[9] For example, zeolitic imidazolate framework particles and ZIF membranes have been synthesized from nanosized ZnO precursors based on this nanoscale-facilitated transformation scheme. Because metal oxide materials can be attached to various substrates, the nanoscale-facilitated transformation is a promising method for synthesizing MOF films from the corresponding nanoscale metal-oxide thin film templates attached on versatile substrates.

This *highlight* focuses on this new method of the nanoscale-facilitated transformation of nanoscopic oxide precursors to the corresponding MOF nanoscopic materials. In this regard, the working principles, fabrications or preparations of MOF membranes, as well as the future goals and directions, will be discussed.

2. MOF nanoparticle fabrication

Zeolite imidazolate frameworks (ZIFs), a new subclass of MOFs, have attracted significant attention because they combine the advantages of both zeolites and conventional MOFs. Most notably, nanosized ZIFs combine the advantages of nanomaterials with the advantageous the properties of the parent ZIF materials,[10] such as enhanced gas storage and catalysis. Although, a number of synthetic methods have been reported for the preparation of nanosized ZIF particles including microemulsions, microwave-assisted routes, surfactant-mediated methods, and sonochemistry, the fabrication of narrowly dispersed nanosized MOF materials is still a very challenging task because of the critical factors required to precisely control the growth conditions of the crystals by these methods.

Significant advances have been made in controlling the size and shape of nanosized MOF particles based on soluble metal salts, such as through direct room temperature solution reactions or solvothermal synthesis utilizing acetic acid to modulate crystallite sizes.[10d,e] Recently, a series of ZIF materials were prepared by direct acid–base reaction between metal oxides or hydroxides and imidazolic ligands under moderate heating.[9a,11] In particular, through the fine-tuning of the thermal reaction conditions, X-ray quality single crystals can be controlled by the addition of small amounts of structure directing agents.[12] Based on this idea, we developed a new method for synthesizing narrowly dispersed ZIF-8 ($Zn(MIM)_2$, HMIM = 2-methylimidazole) particles: an *in situ* approach was used to fabricate nanosized metal oxide (ZnO) precursor seeds that were transformed into ZIF-8 via a nanoscale-facilitated transformation (**Figure 1a,b**).[9a] The key point of this method is that the crystalline ZIF particles grow around the nanosized ZnO precursors; strong stirring inhibits the growth of particles. Compared with the in situ solution method, in which ZIF-8 is fabricated from dissoluble zinc salts, the particle sizes of the products obtained via the nanoscale-facilitated transformation were a littler larger but they show higher uniformity in size and shape, possibly due to a significantly reduced reaction rate when using a metal oxide precursor which is favourable for crystal growth.

While the fact the fabrication of nanosized ZIF-8 particle from dissoluble metal salt precursors appears to be simpler than the nano-scale facilitated transformation method, the *in situ* synthetic method haves three associated drawbacks that lead to a lesser degree of control over nanoparticle sizes: (1) random crystallization of seeds that sometimes results in non-uniform initial nucleation of crystal seeds, (2) difficult control over the speed of crystal growth, and (3) the particles obtained by this method display stronger connecting affinities, resulting in particles adhering to each other. The nanoscale-facilitated transformation method attempts to remedy these issues through tighter control over initial seed crystals. However, unlike the phase pure products obtained from homogeneous solution reactions, the phase purity of the products obtained by the nanoscale-facilitated transformation method is strongly dependent upon the ratio of the ligand HMIM to ZnO precursors: Hexagonally faceted unconsolidated ZIF-8 particles were formed around ZnO particles using an zinc oxide-to-ligand molar ratio of 15:8 (Figure 1a), yet uniform and phase pure ZIF-8 particles were obtained when the molar ratio of HMIM to ZnO was increased to 5:2 (Figure 1b).

Interestingly, during the nanoscale-facilitated transformation of ZnO nanosized precursors to ZIF-8 particles, other nanosized objects, such as multiwall carbon nanotubes (MWNTs), can be easily trapped into the final ZIF-8 particles through the same transformation methodology (**Figure 2**), described as MWNT@ZIF.[9b] The MWNT@ZIF composite can be used as cathode in Li-S batteries where MWNTs are electrically conductive pathways and ZIF-8 particles act as S reservoirs. These MWNT@ZIF composite particles were synthesized simply by adding HMIM to a methanol solution containing ZnO nanoparticles and MWNTs. **Figure 2** contains a schematic, scanning electron microscope (SEM) images, and transmission electron microscopy (TEM) images depicting the formation of MWNT@ZIF composite.

More notably, this facile transformation from ZnO nanoparticles to ZIF-8 particles took place around the ZnO position; therefore this transformation can be further used to make ZIF-8 thin films when the predesigned nanosized ZnO precursors were fixed on special substrates.

3. MOF thin-film fabrications

MOF thin films are employed in a variety of ongoing areas of research, specifically; MOF thin films have been utilized as chemical sensors, separation membranes, and electrode materials.[13] However, the controlled and highly oriented growth of homogenous MOF thin films on a length scale down to molecular dimensions is one of the major challenges in nanotechnology. So far, two methods for MOF membrane fabrication have been developed: an *in situ* synthetic approach and a secondary-growth method. The *in situ* approach is essential to promoting the growth of crystalline material on a support rather than free growth, as shown by Fischer and Bein where an MOF crystalline surface is grown on different functionalized self-assembled monolayers (SAMs).[14] However, the key to the secondary-growth method is to fix small nanosized MOF seeds to a support surface, as demonstrated by Gascon where a HKUST-1 (Hong Kong University of Science and Technology, $[Cu_3(BTC)_2]$·guests, H_3TBC = 1,3,5-benzenetricarboxylic acid) membrane was synthesized on α-alumina by a seeding approach.[15]

3.1 In situ synthetic approach

One major advantage of the *in situ* synthetic approach is its simplicity. This one-step, one-pot method exhibits a facile way to prepare MOF films on either bare or chemically modified supports. In general, seeds are first crystallized and anchored to the substrate directly from solution through a reaction of ligand and metal salts. The MOF crystals are then grown from these seeds and gradually overgrow their neighbors until a continuous MOF film is formed.[16,17]

Although in situ crystallizations appear to be the simpler, and, therefore, the favored preparation route, this approach shows three drawbacks that lead to a lesser degree of control over the initial nucleation of MOF seed crystals: (1) random crystallization of seeds that sometimes results in the formation of cracks on the fully formed membrane, (2) the morphology and the thickness of the membrane are difficult to control, and (3) the MOF crystals obtained by this method display weaker substrate binding affinities, which are of critical importance for practical applications. The secondary growth method attempts to remedy these issues through tighter control over initial seed crystals.

3.2 Secondary growth method

The secondary growth method mainly involves the synthesis and deposition of seed crystals, followed by the crystallization of the seeded support. The most important part of this method is the uniform seeding of the seed crystals on the support prior to the membrane fabrications.[18] Compared to the in situ membrane fabrication method, nucleation and crystal growth of the secondary growth method are two separate steps, and hence nucleation rates and chemical interactions with the supports are less crucial. Therefore, the secondary growth method avoids the seed nucleation problem observed for the *in situ* method.

However, the secondary growth method comes with its own problems. The MOF membranes fabricated by the secondary growth method are highly dependent on the substrates, which determine the nucleation and growth rates. Primarily, the weak adhesion between the substrate and MOF layer can cause films to peel off, especially when accumulated stress is present. In order

to avoid this problem, crack-free MOF membranes can be synthesized by using self-assembled monolayers (SAMs), which has been proven to be a feasible and effective method to control the crystal structure as well as the crystallographic orientation of surface-anchored metal-organic frameworks (SURMOFs) because organic linkers typically do not provide additional linkage groups that can form bonds with linkage groups on the surface of the supports (i.e., hydroxyl groups in case of metal oxides).[19] SAMs must be used to provide strong linkage between the MOFs and support surfaces. After chemical modifications under controlled conditions, highly oriented MOF membranes can be fabricated on SAM interfaces, ideally in a dense, homogeneous and oriented fashion. For example, Hofmann-type clathrate MOF, Fe(pz)[Pt(CN)$_4$] (pz: pyrazine) film on Au/Cr/Si substrate were fabricated using the layer-by-layer (LbL) method, with the substrate soaked in 4-mercaptopyridine solution before alternately treated in the solutions of $Fe(BF_4)_2 \cdot 6H_2O$, $[(C_4H_9)_4N]_2Pt(CN)_4$, and pz. In particular, the orientation of the thin film was highly controlled in both horizontal and vertical directions relative to the substrate (**Figure 3**).[20]

Various substrates and support materials have been used for SAMs, including silica, porous alumina, graphite and organic surfaces, as well as gold.[21] The exposed functional groups of the SAMs can even be designed to specifically interact with the metal ion. Then, the SAM layer takes the role of the linkers by binding and orienting the MOF growth. Most of the MOF films were grown by immersion of the selected substrates into specifically pre-treated solvothermal mother liquors of the particular MOF material. However, the secondary growth method generally requires several step reactions in organic or inorganic acids, washing solvents, and metal salt solutions. These long processes make the overall method expensive and environmentally unfriendly. At the same time, preparation of such thin films, especially highly oriented ones, poses significant difficulties because bulk MOFs are usually made as brittle crystals or insoluble powders that are not amenable to common surface-processing techniques.

The above mentioned nanoscale-facilitated transformation method from nanosized metal oxide precursors can be used for the preparation of MOF membranes. This method combines the advantages of the *in situ* synthetic approach and the secondary growth method, *i.e.*, the one-pot and one-step facile transformation of metal oxide precursors on various substrates that can produce uniform MOF thin films which strongly adhere to the substrates.

3.3 MOF thin-film fabrication from metal oxides

Currently, the preparation of nanoscopic ZnO objects is highly mature and they can readily be prepared on diverse substrates by both solution-based growth methods and chemical vapor deposition (CVD) methods. Meanwhile, due to the enhanced reaction activity of the nanosized ZnO, related ZIF transformation can be done at low temperatures at gram scale, thus, making this method highly advantageous both economically and ecologically.[9] More notably, this nanoscale-facilitated transformation of ZIF particles from ZnO nanoscopic objects has been shown to enable the synthesis of ZIF layers and to overcome the lack of control over the spatial localization of the crystal growth, a typical problem for other approaches. Compared to the layer-by-layer method, this method of starting from layered metal oxide precursors shows almost no restriction regarding the nature of the substrate.

Interestingly, the ZIF membranes can be fabricated by solid-state reactions in which nanoscopic ZnO precursors undergo facile chemical transformations between chemical species without the conventional dissolution process (**Figure 4**).[9a] This synthetic procedure is based on the concepts that substrates coated with metal oxide nanonlayers provide metal ions required for the nucleation and growth of ZIF crystals without any additional surface modifications. In addition, it should be noted that this method of synthesis is optimal for producing highly uniform ZIF nanocrystals. Similarly, based on the solvent-free approach, Ameloot and coworkers synthesized ZIF-8 thin films through the reaction of ZnO films or patterns with melted 2-methylimidazole. Their synthesis approach consists of two simple steps: firstly, ZnO film covered with HMIM ligand powder and melting the ligand powder for in situ solvent-free transformation, then the excess ligand was removed resulting in an evacuated ZIF-8 film (**Figure 5**).[11b] The SEM images of a hexagonal ZIF-8 pattern transformed from ZnO pattern indicate the successful control over the spatial localization of the ZIF crystal growth based upon the transformation from ZnO precursors (**Figure 6**).[11b] This solid state in situ synthetic approach exhibits a facile way to prepare ZIF films on various supports through a film fabrication mechanism. In general, metals oxide nanoparticles are first anchored to the substrate directly from solution-based growth methods and CVD methods. The ZIF crystals are then grown from these tiny precursors and gradually overgrow their neighbors until a continuous ZIF film is developed. Thus this method produces membranes strongly bound to the substrate.

The transformation of ZIF thin films from ZnO nanoscopic objects can be accelerated in a solution. For example, Fischer and co-workers combined atomic layer deposition (ALD) or magnetron sputtering techniques with ZIF thin film fabrication: from ZnO nanolayers to synthesize ZIF-8 thin films.[11e] This technique allows for the self-directed localization of ZIF-8 thin films, as depicted in **Figure 7**. The fabricated ZIF-8 films were coated on silicon (Si/SiO_2) substrates by wet-chemical, microwave-assisted conversion of ZnO layers. Fischer and co-workers developed this method to exert greater control over ZIF-8 thin film porosity and the expected microporosity was deduced from methanol adsorption studies using an environmentally controlled quartz crystal microbalance (QCM). **Figure 8** gave the comparison of the nanosized ZnO precursors and final intergrown polycrystalline ZIF-8 layers with crystal sizes of ~50 nm on the top of Si and QCM substrates.[11e]

As for the method using bare substrates for the MOF membrane fabrication, strong enough interactions between the organic linkers and the surface groups on the substrate are needed. For example, several reports have described the growth and characterization of continuous polycrystalline membranes of materials such as ZIF-7, ZIF-8, ZIF-69, and ZIF-90 on ceramic (α-Al_2O_3, TiO_2) disks and tubular supports based on microwave-assisted method. Because ZnO or Zn surfaces may induce and favor the nucleation of ZIF-8 crystals and possible local crystallizations, ZnO layers can be used as buffers to fabricate ZIF thin films on special substrates. More recently, Zhang and colleagues synthesized strongly adhesive ZIF/PVDF hollow membranes by using a non-activation (NA) ZnO array as a buffer layer (**Figure 9**).[11a] Moreover, the fabricated ZIF/PVDF membranes had hollow fiber structures that are highly pemselective towards H_2. These properties indicate that: (1) NA-ZnO array may be excellent buffering layers for fabricating MOF membranes, and (2) that ZIF/PVDF is a promising material for industrial hydrogen separations. The SEM images of cross-section of the membrane and top view showed that the crystals were anchored to the substrate tightly, no cracks, pinholes, or

other defects on the surface, indicating ZnO layer was found to be vital for membrane formation (**Figure 10**).[11a]

Despite the fact that the nano-facilitate method allows for the fabrication of MOF/ZIF films from inexpensive starting metal oxide materials, affords greater control over the spatial localization of MOF particles during the crystallization process, and promotes the bond connection between film and support; there are disadvantages associated with this method. For instance, the poor activity of other metal oxide nanolayers, such as copper oxide or nickel oxide, inhibits the success of nano-facilitated transformations from these metals. One way around this is to combine nano-facilitated transformation with conventional solution methods. This would be a compensation for the established *in situ* synthetic approach from solutions and secondary-growth method.

4. Summary

Coordination chemistry holds unique prospects for the fabrication of novel functional metal organic framework materials. In particular, the fabrication of crystalline porous films of metal-organic frameworks is highly important for membrane-based separations, membrane reactors, and sensing devices. The fabrication process of crystalline films contains three steps: (1) the organic linkers and metal ions precisely self-assembled together through coordination forces, (2) then the formation of initial MOF seed crystals, and, finally, (3) the assembly of nanosized crystals into two-dimensional well-ordered MOF membranes.

The ability to control the orientation of the crystals and, thus, the pore system in such thin films at the molecular lever will open the way to more advanced applications, such as selective gas-separation membranes or chemical sensors. Although the direct *in situ* synthesis route is a straightforward way to prepare crystalline MOF films, poor bonding to the substrate, poor stability, and macroscopic crack formation in the course of the fabrication process are the main challenges associated with this method. Therefore, many new methods have been developed to improve the quality of the MOF films by seeding or modifying the substrates.

A novel method dubbed the "Dual metal source" method has been explored for membrane formation in which the tiny MOF crystals in the membrane are intergrown together to form a continuous and crack-free layer.[22] Meanwhile, the mechanical strength of MOF membranes can also be increased by the metal oxides substrates as well. In particular, sometimes the dual metal source method can effectively omit the processes of seed preparation and deposition, i.e., the support also acts as a metal source.

The nucleation and, the formation of homogeneous coatings of MOF/ZIF crystals on the substrate surface requires suitable functionalization in the form of in situ growth or through seeding coating (secondary growth) based on SAM-modified or bare substrates, as well as recently developed interfacial synthesis and the direct transformation from metal oxide precursors. The self-completing growth of thin MOF layers based on the interfacial synthesis can not only be used to prepare MOF layers, but also MOF superstructures, such as capsules, when the interfacial growth happens on a droplet surface. The free-standing MOF membranes could have more important applications since they are independent from the substrates. However, methodology based on the nanoscale-facilitated transformation of metal oxide precursors can easily be adapted to synthesize MOF films by attaching the corresponding nanoscale metal oxide thin film templates to versatile substrates. The simplicity of transforming metal oxide precursors on substrates through direct reaction with organic ligands may lead to a wide variety of crystalline films of other MOFs. This method allows for the control of the spatial localization of MOF crystals through the use of inexpensive raw materials.

Given the rich diversity of readily available MOF materials, more MOF membranes with novel functions are anticipated. Future research directions might include new synthesis techniques, tailored microstructure based on an understanding of gas-membrane interactions, the development of MOF membranes responsive to external stimuli, and enhancing gas selectivity/permeance among other practical application.

Acknowledgement

This research was sponsored by the Division of Chemical Sciences, Geosciences, and Biosciences, Office of Basic Energy Sciences, US Department of Energy, under Contract DE-AC05-00OR22725 with Oak Ridge National Laboratory, which is managed and operated by UT-Battelle, LLC.

Notes and references

[a]*Chemical Sciences Division, Oak Ridge National Laboratory, Oak Ridge, Tennessee 37831, USA; E-mail: dais@ornl.gov, yuey@ornl.gov*
[b]*Department of Chemistry, University of Tennessee, Knoxville, Tennessee 37996, USA*

1 (a) L. Ma, C. Abney and W. Lin, *Chem. Soc. Rev.,* 2009, **38**, 1248–1256; (b) O. M. Yaghi, M. O'Keeffe, N. W. Ockwig, H. K. Chae, M. Eddaoudi and J. Kim, *Nature,* 2003, **423**, 705–714; (c) Z. Wang and S. M. Cohen, *Chem. Soc. Rev.*, 2009, **38**, 1315–1329; (d) G. K. H. Shimizu, R. Vaidhyanathan and J. M. Taylor, *Chem. Soc. Rev*., 2009, **38**, 1430–1449; (e) O. K. Farha, C. E. Wilmer, I. Eryazici, B. G. Hauser, P. A. Parilla, K. O'Neill, A. A. Sarjeant, S. T. Nguyen, R. Q. Snurr and J. T. Hupp, *J. Am. Chem. Soc.,* 2012, **134**, 9860–9863.

2 (a) S.-T. Zheng, J. Zhang and G.-Y. Yang, *Angew. Chem. Int. Ed.,* 2008, **47**, 3909–3913; (b) B. Wang, W. Yao, J. Lin, Z. Ding and C. Wang, *Angew. Chem. Int. Ed.*, 2014, **53**, 1034 –1038; (c) A. N. Khlobystov, A. J. Blake, N. R. Champness, D. A. Lemenovskii, A. G. Majouga, N. V. Zyk and M. Schröder, *Coord. Chem. Rev.*, 2001, **222**, 155–192; (d) B. Moulton and M. J. Zaworotko, *Chem. Rev*., 2001, **101**, 1629–1658; (e) J. R. Li, R.-J. Kuppler and H.-C. Zhou,*Chem. Soc. Rev.*, 2009, **38**, 1477–1504.

3 (a) S. T. Zheng, T. Wu, C. T. Chou, A. Fuhr, P. Y. Feng and X. H. Bu, *J. Am. Chem. Soc.,* 2012, **134**, 1934–1937; (b) T. Ben, C. J. Lu, C. Y. Pei, S. X. Xu and S. L. Qiu, *Chem. Eur. J.*, 2012, **18**, 10250–10253; (c) Z.-Q. Li, M. Zhang, B. Liu, C.-Y. Guo and M. Zhou, *Inorg. Chem. Commun*, 2013, **36**, 241–244; (d) W. Zhang and R.-G. Xiong, *Chem. Rev.,* 2012, **112**, 1163–11195; (e) H. Furukawa, N. Ko, Y. B. Go, N. Aratani, S. B. Choi, E. Choi, A. Ö. Yazaydin, R. Q. Snurr, M. O'Keeffe, J. Kim and O. M. Yaghi, *Science*, 2010, **329**, 424–428; (f) K. Konstas, T. Osl, X. Yang, M. Batten, N. Burke, A. J. Hill and M. R. Hill, *J. Mater. Chem*., 2012, **22**, 16698–16708; (g) H. Wu, H. Gong, D. H. Olson and J. Li, *Chem. Rev*. 2012, **112**, 836–868.

4 (a) W.-Y. Gao, Y. Chen, Y. Niu, K. Williams, L. Cash, P. J. Perez, L. Wojtas, J. Cai, Y.-S. Chen and S. Ma, *Angew. Chem. Int. Ed*., 2014, **53**, 2615–2619; (b) A. Sonnauer, F. Hoffmann, M. Fröba, L. Kienle, V. Duppel, M. Thommes, C. Serre, G. Férey and N. Stock, *Angew. Chem. Int. Ed.,* 2009, **48**, 3791–3794; (c) D. M. D'Alessandro, B. Smit and J. R. Long, *Angew. Chem. Int. Ed.,* 2010, **49**, 6058–6082; (e) W. M. Bloch, R. Babarao, M. R. Hill, C. J. Doonan and C. J. Sumby, *J. Am. Chem. Soc.,* 2013, **135***,* 10441–10448; (f) M. C. Das,

H. Xu, Z. Wang, G. Srinivas, W. Zhou, Y. Yue, V. N. Nesterov, G. Qian and B. Chen, *Chem. Comm*., 2011, **47**, 11715–11717.

5 (a) L. E. Kreno, K. Leong, O. K. Farha, M. Allendorf, R. P. Van Duyne and J. T. Hupp, *Chem. Rev*., 2012, **112**, 1105–1125; (b) Y. Yue, A. J. Binder, R. Song, Y. Cui, J. Chen, D. K. Hensley and S. Dai, *Dalton Trans*., 2014, **43**, 17893–17898.

6 (a) W. Morris, W. E. Briley, E. Auyeung, M. D. Cabezas and C. A. Mirkin, *J. Am. Chem. Soc*., 2014, **136**, 7261−7264; (b) A. Carné-Sánchez, I. Imaz, M. Cano-Sarabia and D. Maspoch, *Nature Chem*., 2013, **5**, 203–211; (c) G. Lu, S. Li, Z. Guo, O. K. Farha, B. G. Hauser, X. Qi, Y. Wang, X. Wang, S. Han, X. Liu, J. S. DuChene, H. Zhang, Q. Zhang, X. Chen, J. Ma, S. C. J. Loo, W. D. Wei, Y. Yang, J. T. Hupp and F. Huo, *Nature Chem*., 2012, **4**, 310–316; (d) D. H. Lee, S. Kim, M. Y. Hyun, J.-Y. Hong, S. Huh, C. Kim and S. Lee, J. *Chem. Commun*., 2012, **48**, 5512–5514.

7 (a) S. Hermes, F. Schröder, R. Chelmowski, C. Wöll and R. A. Fischer, *J. Am. Chem. Soc.,* 2005, **127**, 13744–13745; (b) D. Zacher, A. Baunemann, S. Hermes and R. A. Fischer, *J. Mater. Chem*., 2007, **17**, 2785–2792; (c) D. Zacher, O. Shekhah, C. Wöllb and R. A. Fischer, *Chem. Soc. Rev*., 2009, **38**, 1418–1429; (d) Z. Dou, J. Yu, H. Xu, Y. Cui, Y. Yang and G. Qian, *Thin Solid Films*, 2013, **544**, 296–300; (e) Y. Yoo and H.-K. Jeong, *Chem. Commun*., 2008, 2441–2443; (f) H. T. Kwon and H.-K. Jeong, *Chem. Commun*., 2013, **49**, 3854–3856; (g) Z.-Q. Li, M. Zhang, B. Liu, C.-Y. Guo, M. Zhou, *Inorg. Chem. Commun*., 2013, **36**, 241–244; (h) A. Centrone, Y. Yang, S. Speakman, L. Bromberg, G. C. Rutledge, T. A. Hatton, *J. Am. Chem. Soc*., 2010, **132**, 15687−15691.

8 (a) J.-R. Li, J. Sculley and H.-C. Zhou, *Chem. Rev*., 2012, **112**, 869–932; (b) M. Shah, M. C. McCarthy, S. Sachdeva, A. K. Lee and H.-K. Jeong, *Ind. Eng. Chem. Res*., 2012, **51**, 2179–2199; (c) A. Bétard and R. A. Fischer, *Chem. Rev*., 2012, **112**, 1055–1083; (d) M. Arnold, P. Kortunov, D. J. Jones, Y. Nedellec, J. Kaerger and J. Caro, *Eur. J. Inorg. Chem*., 2007, 60–64; (e) S. Qiu, M. Xue and G. Zhu, *Chem. Soc. Rev*., 2014, **43**, 6116–6140.

9 (a) Y. Yue, Z.-A. Qiao, X. Li, A. J. Binder, E. Formo, Z. Pan, C. Tian, Z. Bi, S. Dai, *Cryst. Growth Des*., 2013, **13**, 1002−1005; (b) Y. Yue, B. Guo, Z.-A. Qiao, P. F. Fulvio, J. Chen, A. J. Binder, C. Tian and S. Dai, *Microporous Mesoporous Mater*., 2014, **198**, 139–143.

10 (a) J. P. Zhang, Y. B. Zhang, J. B. Lin and X. M. Chen, *Chem. Rev*., 2012, **112**, 1001–1033; (b) M. Asta, B. B. Laird, O. M. Yaghi, *J. Am. Chem. Soc.* **2010**, *132*, 11006–11008; (c) M. J. Cliffe, C. Mottillo, R. S. Stein, D. K. Bučar and T. Friščić, *Chem. Sci.,* 2012, **3**, 2495–2500; (d) Y. Pan, Y. Liu, G. Zeng, L. Zhao and Z. Lai, *Chem. Commun*., 2011, **47**, 2071–2073; (e) W. Morris, W. E. Briley, E. Auyeung, M. D. Cabezas and C. A. Mirkin, *J. Am. Chem. Soc*., 2014, **136**, 7261−7264.

11 (a) W. Li, Q. Meng, X. Li, C. Zhang, Z. Fan and G. Zhang, *Chem. Commun*., 2014, **50**, 9711–9713; (b) I. Stassen, N. Campagnol, J. Fransaer, P. Vereecken, D. D. Vos and R.Ameloot, *CrystEngComm*, 2013, **15**, 9308–9311; (c) H. Guo, G. Zhu, I. J. Hewitt and S. Qiu, *J. Am. Chem. Soc*., 2009, **131**, 1646–1647; (d) J. Liu, F. Sun, F. Zhang, Z. Wang, R. Zhang, C. Wang and S. Qiu, *J. Mater. Chem*., 2011, **21**, 3775–3778; (e) K. Khaletskaya, S. Turner, M. Tu, S. Wannapaiboon, A. Schneemann, R. Meyer, A. Ludwig, G. Van Tendeloo and R. A. Fischer, *Adv. Funct. Mater*. 2014, DOI: 10.1002/adfm.201400559.

12 M. Lanchas, D. Vallejo-Sánchez, G. Beobide, O. Castillo, A. T. Aguayo, A. Luquea and P. Román, *Chem. Commun*., 2012, **48**, 9930–9932.

13 (a) Y. Wu, F. Li, H. Liu, W. Zhu, M. Teng, Y. Jiang, W. Li, D. Xu, D. He, P. Hannam and G. Li, *J. Mater. Chem*., 2012, **22**, 16971–16978; (b) E. Redel, Z. Wang, S. Walheim, J. Liu, H. Gliemann and C. Wöll, *Appl. Phys. Lett*., 2013, **103**, 091903; (c) V. Stavila, J. Volponi, A. M. Katzenmeyer, M. C. Dixonb and M. D. Allendorf, *Chem. Sci*., 2012, **3**, 1531–1540; (d) E. A. Flügel, A. Ranft, F. Haase and Bettina V. Lotsch, *J. Mater. Chem.,* 2012, **22**, 10119–10133.

14 (a) A. Schoedel, C. Scherb and T. Bein, *Angew. Chem. Int. Ed*., 2010, **49**, 7225–7228; (b) S. Hermes, D. Zacher, A. Baunemann, C. Wöll and R. A. Fischer, *Chem. Mater*., 2007, **19**, 2168–2173; (c) O. Shekhah, H. Wang, S. Kowarik, F. Schreiber, M. Paulus, M. Tolan, C. Sternemann, F. Evers, D. Zacher, R. A. Fischer and C. Wöll, *J. Am. Chem. Soc*., 2007, **129**, 15118–15119.

15 J. Gascon, S. Aguado and F. Kapteijn, *Microporous Mesoporous Mater*., 2008, **113**, 132–138.

16 (a) D. Zacher, A. Baunemann, S. Hermes and R. A. Fischer, *J. Mater. Chem*., 2007, **17**, 2785–2792; (b) D. Zacher, O. Shekhah, C. Wöllb and R. A. Fischer, *Chem. Soc. Rev*., 2009, **38**, 1418–1429.

17 (a) Z. Dou, J. Yu, H. Xu, Y. Cui, Y. Yang and G. Qian, *Thin Solid Films*, 2013, **544**, 296–300; (b) Y. Yoo and H.-K. Jeong, *Chem. Commun*., 2008, 2441–2443.

18 (a) H. Bux, A. Feldhoff, J. Cravillon, M. Wiebcke, Y.-S. Li and J. Caro, *Chem. Mater*., 2011, **23**, 2262–2269; (b) A. Bétard, S. Wannapaiboon and R. A. Fischer, *Chem. Commun*., 2012, **48**, 10493–10495; (c) Z. Wang, J. Liu, H. K. Arslan, S. Grosjean, T. Hagendorn, H. Gliemann, S. Bräse and C. Wöll, *Langmuir*, 2013, **29**, 15958−15964; (d) J. Nan, X. Dong, W. Wang, W. Jin and N. Xu, *Langmuir*, 2011, **27**, 4309–4312.

19 S. Bundschuh, O. Kraft, H. K. Arslan, H. Gliemann, P. G. Weidler and C. Wöll, *Appl. Phys. Lett*., 2011, **101**, 101910.

20 K. Otsubo, T. Haraguchi, O. Sakata, A. Fujiwara and H. Kitagawa, *J. Am. Chem. Soc*., 2012, **134**, 9605−9608.

21 (a) E. Biemmi, C. Scherb and T. Bein, *J. Am. Chem. Soc.,* 2007, **129**, 8054–8055; (b) C. Hou, Q. Xu, J. Peng, Z. Ji and X. Hu, *ChemPhysChem*, 2013, **14**, 140–144; (c) J.-L. Zhuang, D. Ceglarek, S. Pethuraj and A. Terfort, *Adv. Funct. Mater.*, 2011, **21**, 1442–1447.

22 (a) S. Zhou, X. Zou, F. Sun, H. Ren, J. Liu, F. Zhang, N. Zhao and G. Zhu, *Int. J. Hydrogen Energy*, 2013, **38**, 5338–5347; (b) H. Guo, G. Zhu, I. J. Hewitt and S. Qiu, *J. Am. Chem. Soc*., 2009, **131**, 1646–1647; (c) J. Liu, F. Sun, F. Zhang, Z. Wang, R. Zhang, C. Wang and S. Qiu, J. Mater. Chem., 2011, **21**, 3775–3778.

A table of contents entry

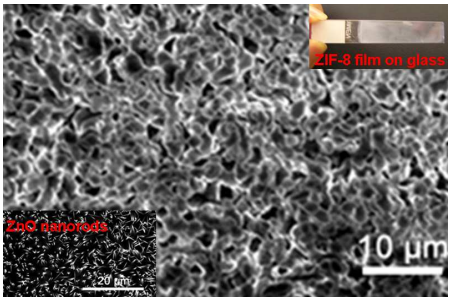

Metal-organic framework films were fabricated on versatile substrates through the nanoscale-facilitated transformation of nanoscopic metal-oxide precursors.

Figure 1. (a) TEM image of unconsolidated ZIF-8 particles with some remaining ZnO particles (molar ration of HMIM to ZnO is15:8); (b) Schematic illustration of the formation of ZIF-8 particles with different ratio of HMIM to ZnO precursors. Reprinted with permission from ref. 9a. Copyright (2013) American Chemical Society.

Figure 2. (a) Schematic of the formation of MWNT@ZIF-8 composites with I-V representing the gradual consumption of ZnO by HMIM; (b) SEM image of MWNT@ZIF composite with an inset showing the scanning electron microscope (SEM) image with a higher magnification; (c) transmission electron microscopy (TEM) image of MWNT@ZIF composite; (d) SEM image and (e) TEM image of MWNT@ZIF composite with ZnO residues in the ZIF-8 particles. Reprinted from ref. 9b, Copyright (2014), with permission from Elsevier.

Figure 3. Schematic representation of the step-by-step approach to fabricating $Fe(pz)[Pt(CN)_4]$ thin film, proposed by Otsubo and co-workers. Reprinted with permission from ref. 20. Copyright (2012) American Chemical Society.

Figure 4. (a) SEM image of the ZnO nanorods on a Si substrate, (b) SEM images of ZIF-8 film on a Si wafer transformed from ZnO nanorods. Reprinted with permission from ref. 9a. Copyright (2013) American Chemical Society.

Figure 5. Schematic overview proposed by Ameloot and coworkers of the solvent-free ZIF-8 film processing and patterning approach. Reproduced from ref. 11b with permission from The Royal Society of Chemistry.

Figure 6. SEM images of a hexagonal ZIF-8 pattern transformed from ZnO pattern, scale bars: 20 μm (a) a high magnification view of the sharp edge, scale bar 1 μm (b). Reproduced from ref. 11b with permission from The Royal Society of Chemistry.

Figure 7. Schematic of the two methods for fabricating ZIF-8 thin films proposed by Fischer and co-workers. Reproduced with permission from ref 11e. Copyright 2014 Wiley-VCH.

Figure 8. SEM images of (a) ZIF-8 derived from sputtered ZnO on a Si substrate, (b) ZIF-8 derived from ALD-ZnO on a Si substrate, (c) ZIF-8 derived from sputtered ZnO on QCM sensor and (d) ZIF-8 derived from ALD-ZnO on QCM sensor. Reproduced with permission from ref 11e. Copyright 2014 Wiley-VCH.

Figure 9. Schematic of the morphology *(left)* and chemical structure *(right)* of ZIF/PVD membranes. Reproduced from ref. 11a with permission from The Royal Society of Chemistry.

Figure 10. Cross-section (a) and surface (b) SEM images of ZIF-8/PVDF membrane. Reproduced from ref. 11a with permission from The Royal Society of Chemistry.

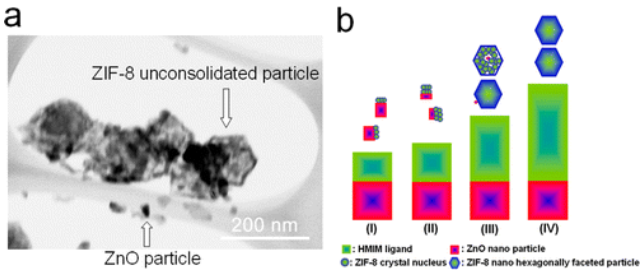

Figure 1. (a) TEM image of unconsolidated ZIF-8 particles with some remaining ZnO particles (molar ration of HMIM to ZnO is15:8); (b) Schematic illustration of the formation of ZIF-8 particles with different ratio of HMIM to ZnO precursors. Reprinted with permission from ref. 9a. Copyright (2013) American Chemical Society.

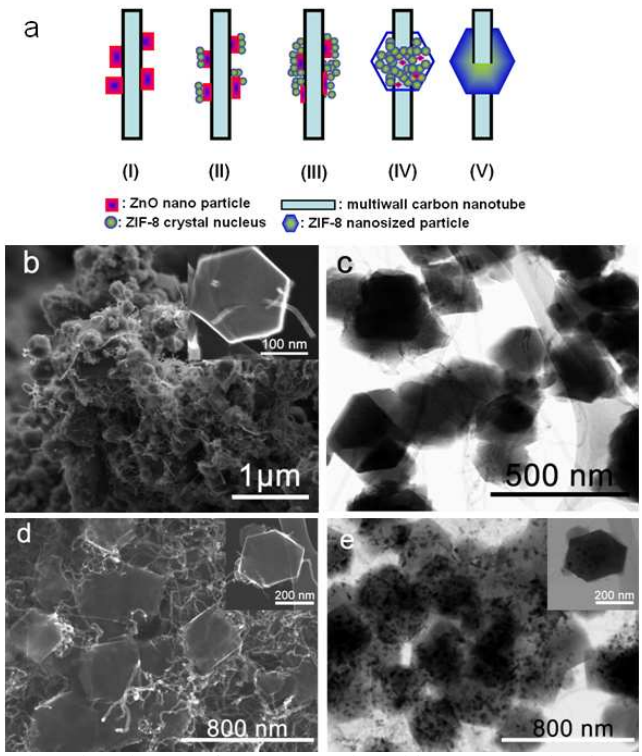

Figure 2. (a) Schematic of the formation of MWNT@ZIF-8 composites with I-V representing the gradual consumption of ZnO by HMIM; (b) SEM image of MWNT@ZIF composite with an inset showing the scanning electron microscope (SEM) image with a higher magnification; (c) transmission electron microscopy (TEM) image of MWNT@ZIF composite; (d) SEM image and (e) TEM image of MWNT@ZIF composite with ZnO residues in the ZIF-8 particles. Reprinted from ref. 9b, Copyright (2014), with permission from Elsevier.

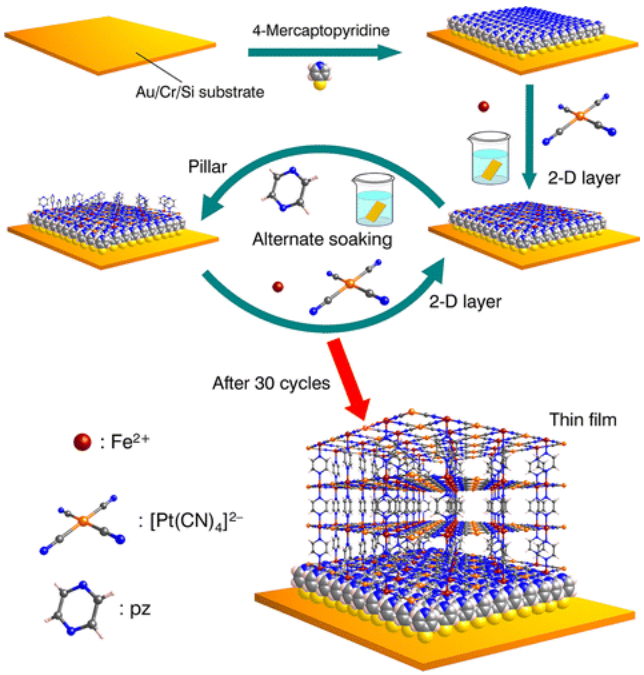

Figure 3. Schematic representation of the step-by-step approach to fabricating Fe(pz)[Pt(CN)$_4$] thin film, proposed by Otsubo and co-workers. Reprinted with permission from ref. 20. Copyright (2012) American Chemical Society.

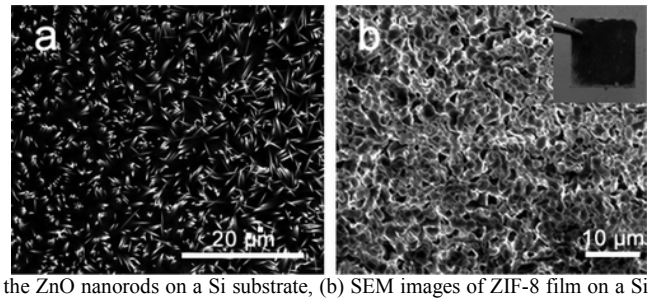

Figure 4. (a) SEM image of the ZnO nanorods on a Si substrate, (b) SEM images of ZIF-8 film on a Si wafer transformed from ZnO nanorods. Reprinted with permission from ref. 9a. Copyright (2013) American Chemical Society.

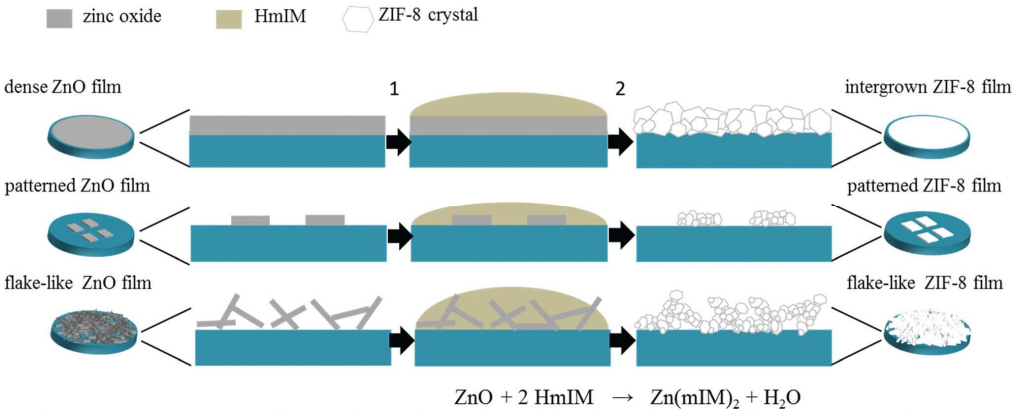

Figure 5. Schematic overview proposed by Ameloot and coworkers of the solvent-free ZIF-8 film processing and patterning approach. Reproduced from ref. 11b with permission from The Royal Society of Chemistry.

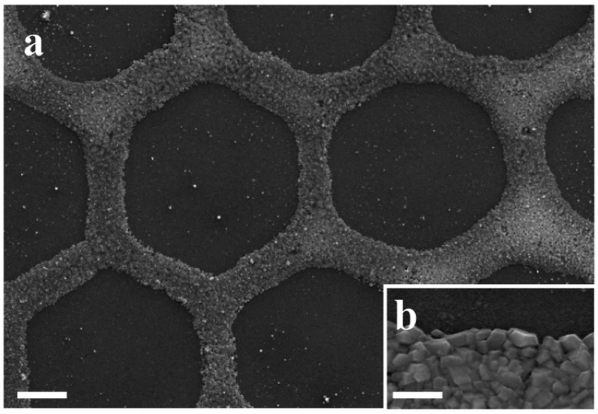

Figure 6. SEM images of a hexagonal ZIF-8 pattern transformed from ZnO pattern, scale bars: 20 μm (a) a high magnification view of the sharp edge, scale bar 1 μm (b). Reproduced from ref. 11b with permission from The Royal Society of Chemistry.

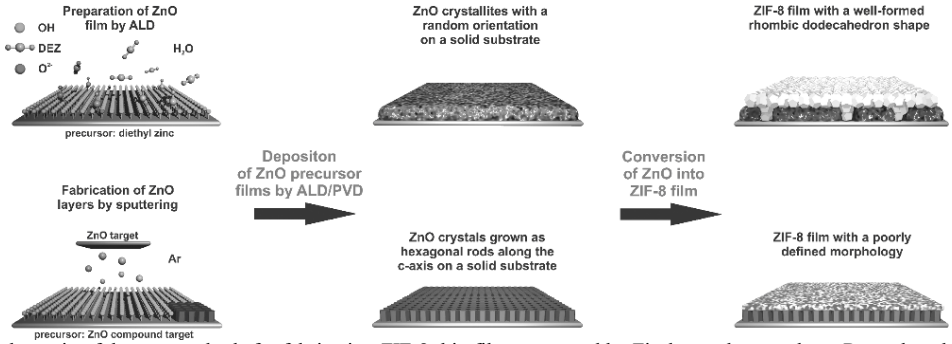

Figure 7. Schematic of the two methods for fabricating ZIF-8 thin films proposed by Fischer and co-workers. Reproduced with permission from ref 11e. Copyright 2014 Wiley-VCH.

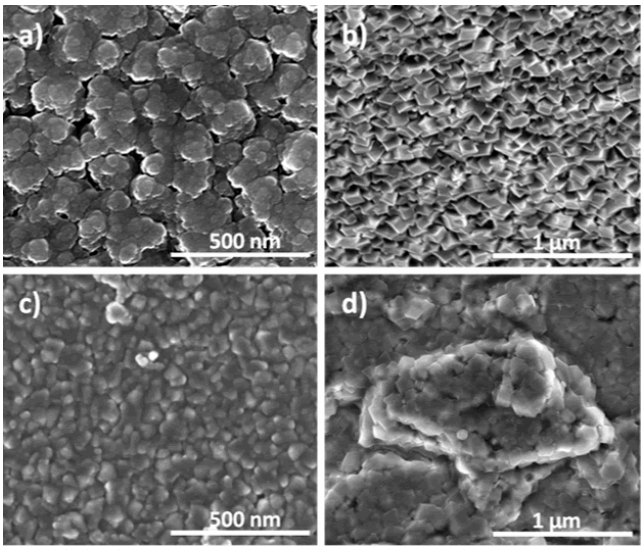

Figure 8. SEM images of (a) ZIF-8 derived from sputtered ZnO on a Si substrate, (b) ZIF-8 derived from ALD-ZnO on a Si substrate, (c) ZIF-8 derived from sputtered ZnO on QCM sensor and (d) ZIF-8 derived from ALD-ZnO on QCM sensor. Reproduced with permission from ref 11e. Copyright 2014 Wiley-VCH.

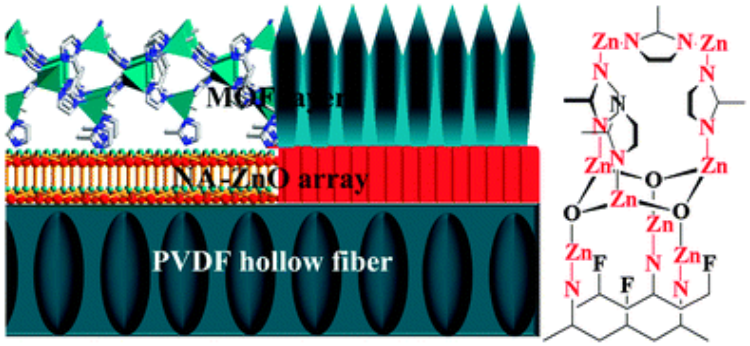

Figure 9. Schematic of the morphology *(left)* and chemical structure *(right)* of ZIF/PVD membranes. Reproduced from ref. 11a with permission from The Royal Society of Chemistry.

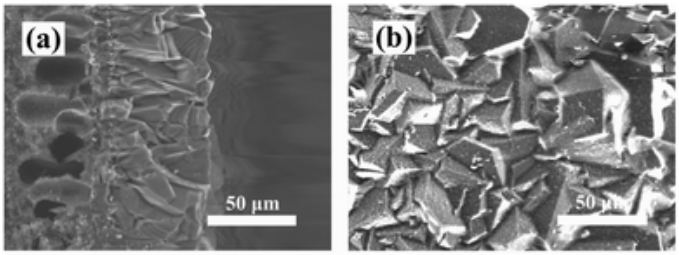

Figure 10. Cross-section (a) and surface (b) SEM images of ZIF-8/PVDF membrane. Reproduced from ref. 11a with permission from The Royal Society of Chemistry.